# Dynamical Climatology

## Intermediate models of intraseasonal and interannual waves in the tropics.

by

G.R. Budin and M.K. Davey

DCTN 83

October 1989

Meteorological Office (Met. O. 20)
London Road
Bracknell
Berkshire RG12 2SZ

Dynamical Climatology Technical Note No. 83

# INTERMEDIATE MODELS OF INTRASEASONAL AND INTERANNUAL WAVES IN THE TROPICS

by

**G.R. Budin**

Hooke Institute for Atmospheric Research, Oxford

and

**M.K. Davey**

Met O 20 (Dynamical
Climatology Branch)
Meteorological Office
London Rd
Bracknell
Berkshire, U.K. RG12 2SZ

October 1989

Note: This paper has not been published. Permission to quote from it should be obtained from the Assistant Director of the above Meteorological Office Branch.

ABSTRACT

In this paper we describe a coupled ocean-atmosphere-land model of intermediate complexity, with realistic tropical geometry. We find that land conditions control whether or not the model produces interannual variability in the Pacific; a result which emphasises the importance of the 'maritime continent' region in affecting tropical variability. Active interannual variability is confined to the Pacific region, with eastward propagation of coupled modes that are regenerated in the western Pacific at regular intervals. Additional atmospheric 'noise' in the 9 to 180 day range , and an annual cycle in land heating, did not disturb this regular behaviour.

## INTRODUCTION

The main interannual signal in the tropics is the El Niño Southern Oscillation (ENSO) phenomenon, which is essentially driven by ocean-atmosphere interaction in the Pacific (and probably Indian Ocean) regions. In this paper a tropical ocean-atmosphere model of intermediate complexity, incorporating a limited set of physical processes, is used to investigate variability up to interannual timescales. The prognostic model atmosphere has a single vertical mode and an explicit moisture budget, while the ocean has one active upper layer incorporating simple thermodynamics. The model extends around the globe up to 30° each side of the equator on an equatorial $\beta$ plane, with a realistic land-ocean distribution. A constant non-latent heating component is used over land and land dryness is taken into account in the moisture budget. Using this model we aim to address several aspects of ENSO.

Most analyses of intermediate coupled models have focussed on the interaction of the ocean and atmosphere over the Pacific (eg Battisti 1988, 1989a and 1989b, Hirst 1986 and 1988, Hirst and Lau 1989, Zebiak and Cane 1987, Battisti and Hirst 1989). While these papers have provided a useful insight into coupled processes as interactions of the ocean and atmosphere, it has been suggested that atmospheric heating over land, notably that associated with the convective heating of the Asian-Australian monsoon system, may also fundamentally influence events over the Pacific (see Philander and Rasmusson 1985 , Anderson and McCreary 1985a and 1985b, Yamagata and Masumoto 1989). Here we examine such effects in a simple coupled model which includes very crudely the major tropical land masses. Additionally, we aim to see if the observed tropical quasi-biennial oscillation (Yasunari 1985, Rasmusson, personal communication) can be reproduced in the present model.

In addition to the tropical ENSO signal, a major signal found in the tropical atmosphere is that of intraseasonal ('30 to 60 day') eastward propagating waves. This activity is somewhat irregular and has been shown to fluctuate in a manner partly related to ENSO events (Mehta and Krishnamurti 1988, Lau and Chan 1988, and Gray 1988). ENSO and the intraseasonal oscillation share the property that deep convection and the associated latent heat release is an important ingredient of their dynamical behaviour (Lau and Chan 1986, and Lau and Shen 1988). The question arises as to whether the intraseasonal oscillation can perturb the ENSO cycle, as suggested by Lau (1985), Lau and Chan (1986 and 1988), Lau *et. al.* (1989) and others. As a first step to investigating the interaction of intraseasonal and interannual waves we include here some results from the intermediate tropical ocean-atmosphere-land model with a random forcing component added to the atmosphere. In 'aquatropic' experiments with the atmospheric model alone the random forcing produces moist Kelvin waves which resemble the intraseasonal oscillation (Davey, 1989). Here we look at the effect of this forcing in the coupled system with a realistic land-ocean distribution.

## DESCRIPTION OF THE MODEL

A brief outline of the basic equations is provided in this section: for a more complete description see Anderson and McCreary (1985a) for the ocean, Davey and Gill (1987) for the atmosphere, and Budin and Davey (1989) for details of the coupled model. The domain for this model spans 360° around the globe, from 30°N to 30°S. The model ocean has $1° \times 1°$ latitude-longitude resolution and uses a 3 hour timestep, while the atmosphere has $4° \times 4°$ resolution and a 20 minute timestep, both on a C-grid. Extra damping at the closed northern and southern ocean boundaries is provided to eliminate undesirable coastal Kelvin waves.

*Oceanic component*

The tropical ocean is represented by a single active layer with depth $h$ and temperature $T$ overlying a passive deep layer with constant temperature $T_o$ and density $\rho_o$. In flux form, the horizontal nonlinear equations of motion for the active layer on an equatorial beta-plane are

$$(hu)_t + \nabla.(hu\underline{u}) - fhv = (X - P_x)/\rho_o + \nu_o \nabla^2 (hu), \tag{1a}$$

$$(hv)_t + \nabla.(hv\underline{u}) + fhu = (Y - P_y)/\rho_o + \nu_o \nabla^2 (hv), \tag{1b}$$

where $\underline{u} = (u,v)$ is horizontal velocity, $P = \rho_o \alpha\, gh^2\,(T - T_o)/2$ is potential energy, and $f = \beta y$ is the Coriolis parameter. The wind stress is

$$(X,Y) = D\,(U,V), \tag{2}$$

proportional to the surface wind $\underline{U}$.

Temperature and depth vary according to

$$T_t + \underline{u}.\nabla T = -2\,[\gamma(T - T^*) + \delta_o/h^2]\,/\,h + \nu_o \nabla^2 T, \tag{3}$$

$$h_t + \nabla.(h\underline{u}) = [\gamma\,(T - T^*) + 2\delta_o/h^2\,]\,/\,(T - T_o) - \omega_o. \tag{4}$$

The term $\gamma(T - T^*)$ is a Haney-type heat flux representing the net effect of solar input, and evaporative, sensible and radiative cooling. The effective temperature $T^*$ (always larger than $T$) is constant in time, with the form

$$T^* = 30.6 - 7.9 \sin^2 (\pi y/2y_o),$$

which is largest at the equator and decreases to the boundaries at $y = \pm y_o$. The term involving the constant $\delta_o$ represents wind mixing that tends to deepen and cool the

upper layer, while $\omega_o$ is a constant background upwelling that counteracts the deepening and also provides a heat sink to offset the surface heat input. The various constants are listed in Table 1. Note that for a depth of 100 m the time scale for temperature change by the Haney forcing is about 200 days.

The oceanic gravity wave speed is

$$c = [\, \alpha\, g\, (T - T_o) h\, ]^{\frac{1}{2}},$$

which varies with position and time. A typical value is about 1.4 m/sec. From Eqns. (3) and (4), in the absence of motion and diffusion the ocean reaches local thermodynamic equilibrium with temperature $\bar{T}$ and depth $\bar{h}$ given by

$$\bar{T} = T_o + \gamma\, (T^* - T_o)/(\gamma + \omega_o), \tag{5a}$$

$$\bar{h} = [\delta_o/\omega_o(\bar{T} - T_o)]^{\frac{1}{2}} \tag{5b}$$

For the parameters chosen, $\bar{T}$ ranges from 29° at the equator to 22°C at $y = \pm y_o$, while $\bar{h}$ increases poleward from 75 m to 100 m. These analytic values are used as initial conditions in the numerical experiments described in later sections.

*Atmospheric component*

The atmosphere has the vertical structure of a single baroclinic mode, between the sea surface at $z = 0$ to a rigid lid at the tropopause at $z = \pi H$, and has a constant background buoyancy frequency. The linear equations of motion are

$$U_t - fV = -p_x/\rho_{oo} - \varepsilon U + \nu_a\, \nabla^2\, U, \tag{6a}$$

$$V_t + fU = -p_y/\rho_{oo} - \varepsilon V + \nu_a\, \nabla^2\, V, \tag{6b}$$

where $p$ is the surface pressure perturbation. The constants $\varepsilon$ etc. are provided in Table 2. The mid-level potential temperature perturbation $\theta$ is controlled by

$$\theta_t + W(\theta_z)_{oo} = \varepsilon(\theta_s + \theta_R - \theta) + \nu_a \nabla^2 \theta + m\, Pr, \tag{7}$$

where $(\theta_z)_{oo}$ is the constant background potential temperature gradient scale. The mid-level vertical velocity $W$ is related to the low-level wind (U,V) by

$$U_x + V_y + W/H = 0\,. \tag{8}$$

Over oceans, the term $\theta_s$ in Eqn. (7) represents heating directly related to the underlying sea surface temperature $T$ ($^\circ C$), with

$$\theta_s = T - 26.5\,, \tag{9}$$

while $\theta_R$ is an additional random heating that may be added to represent processes not explicitly included in the model. Circulation dependent latent heating is included in the form $mPr$, where $Pr$ is a precipitation rate (see below) and $m$ is a constant conversion factor. The link between Eqns. (6) and (7) is that $p$ is related to $\theta$ by

$$p/\rho_{oo} = -gH\ \theta/\theta_{oo} \tag{10}$$

In this system the speed of a dry gravity wave is

$$C = [g(\theta_z)_{oo}/\theta_{oo}]^{\frac{1}{2}}\ H$$

which is about 60 m/sec for the atmospheric parameters listed in Table 2.

The precipitation rate is determined by a moisture budget whereby changes are partitioned between precipitation $Pr$ and column moisture $q$ according to

$$q_t = (1-\sigma)R\ ,\ \ Pr = \sigma\, R \tag{11}$$

where

$$R = -\nabla \cdot (\underline{U} q) + E + v_a \nabla^2 q \tag{12}$$

is the result of low-level convergence, evaporation and diffusive effects, and

$$\sigma = \begin{cases} (q - q_c)/(q_s - q_c) & \text{if } R > 0 \text{ and } q > q_c, \\ 0 & \text{otherwise} \end{cases} \tag{13}$$

Here $q_s$ is the saturation moisture content, which depends on sea surface temperature T by

$$q_s = q_s\,(27) \quad \exp\{\, 0.06(T - 27)\,\}\,. \tag{14}$$

The threshold value for the onset of precipitation is $q_c = 0.8\, q_s$ (a relative humidity of 80% ). Evaporation $E$ in Eqn. (12) depends on wind speed, with

$$E = (\, E_o + E_v \,|\, \underline{U} \,|\,) \begin{cases} q_s - q & \text{if } q < q_c \\ q_s - q_c & \text{if } q > q_c \end{cases} \tag{15}$$

The latent heating effectively reduces the atmospheric static stability to moist values, and hence reduces wave speeds. For example, in a region of active latent heating over a sea surface with $T = 27°C$ wave speeds are approximately half those found in the absence of latent heating.

*Land effects*

Over land we use a very simple atmospheric non-latent heating term, setting

$$\theta_s = T_e - 26.5, \tag{16}$$

(similar to Eqn. (9) for heating over oceans), where now $T_e$ is an 'effective' land surface temperature. In reality $T_e$ encompasses a balance of many thermodynamic and

dynamic processes; solar and long-wave radiation, land heat storage, turbulent heat transfer, etc. The details of these are beyond the scope of the present model. In this paper we simply set $T_e$ to be constant and look at the effect of choosing various values. In Eqn. 7 $\epsilon(\theta_s - \theta)$ acts as a small background forcing which can trigger the (interactive) large latent heating, $mPr$. We are interested in the effects of the location of this latent heating on the model behaviour.

Surface dryness is taken into account by using a 'bucket' model over land . Here evaporation is modified by a moisture availability factor, $SM/SM_d$ where $SM$ is the soil moisture given by the integral of the flux of surface water

$$SM = \int (Pr - E)dt$$

and $SM_d$ is the maximum soil moisture, above which value all precipitation 'runs off' and is lost from the model.

## RESULTS FOR VARIOUS VALUES OF $T_e$

In this section we examine the effects of varying the land conditions: land cooling (Case I), neutral land (Case II) , and land heating (Case III), corresponding to an effective land temperature of $T_e$ equal to $24.5°C$ , $26.5°C$, and $28.5°C$, respectively. (All experiments in this paper are summarized in Table 3.) The term $\epsilon\theta_s$ in the atmospheric heat equation (7) gives a land cooling perturbation of about $0.9°C/day$ for Case I, no land heating for Case II, and a land heating perturbation of $0.9°C/day$ for Case III.

In each case the atmospheric model is initially run alone for 15 days, by which time moist processes are fully spun up and the atmosphere is in equilibrium with the initial SST and land heating distribution. Following this warm-up period the models are coupled.

Figs. 1 - 3 show the development of near-equatorial precipitation for Cases I to III, respectively. For Case I (Fig. 1) there are initially a few weak eastward moving damped inter-annual oscillations in the Pacific region only, and after about 10 years a steady state is effectively reached, with precipitation spread across the Pacific with a strong maximum in the eastern Pacific. There is also rainfall of comparable magnitude over the Indian and mid-Atlantic oceans, but the land is dry. For Case II (Fig. 2) regular oscillations in the Pacific appear, with some small associated fluctuations in the Atlantic and Indian oceans. The period of the oscillation is 6.2 years, with the disturbance propagating eastward across the Pacific in 2.5 years and then lingering in the east Pacific before regenerating in the western Pacific. Rainfall is much stronger in the Pacific than in the Case I equilibrium state, but weaker in the Atlantic and Indian oceans. There is no rainfall over land in Fig. 2. Close examination of other model fields (not shown here) reveals a consistent eastward propagating mode at all latitudes, as in Hirst (1988). There are no westward propagating free ocean waves of the type found by Battisti (1988). For Case III (Fig. 3) with heating over land the model once more reaches a steady state, this time with the largest precipitation in the western Pacific, and precipitation now over the land as well. There are no transient oscillations in the Pacific, but there is initial slow eastward propagation of a disturbance from the Atlantic, which travels across a wet African region through the Indian Ocean to the west Pacific before it dies out.

Figs. 4 - 6 give the geographical distribution of SST and precipitation after 20 model years of integration for Cases I to III, respectively. Note that as land heating is increased precipitation tends to move from over the oceans to be over or near land, and that over the oceans precipitation is concentrated over regions of highest SST. Also as land heating is increased the main precipitation belts over the Pacific shift off the equator, associated with the development and deepening of an equatorial cold tongue.

For Case I the warmest water is in the east Pacific, underlying the largest precipitation. Note that there is a dry area in the extreme east Pacific which is due to dry easterly winds coming off the land (see Fig. 7, described later). Fig. 5 for the oscillating Case II shows a phase when warm SST and strong rainfall has reached the eastern Pacific, and SST and rainfall are increasing in the west Pacific. Note that unlike Case I the central Pacific is cool at this time.

Fig. 6 (Case III) looks like the cold ENSO Pacific state (La Niña) : a warm west Pacific with SST above $29°C$ near the 'maritime continent' (with associated maximum precipitation), and cool SST in the central Pacific (with no rainfall). There are rainbands either side of the equator like a double 'Inter-Tropical Convergence Zone'. The large precipitation in the west Pacific drives the easterly wind over much of the equatorial Pacific. This wind forces a shallow thermocline and cool SST (due to the influence of upwelled water) throughout the central and eastern Pacific. The easterly wind also gives a deep thermocline and warm SST in the west Pacific. Outside the Pacific for Case III (Fig. 6) there is an area of large precipitation extending from across equatorial Africa into the western Indian ocean, and a further large rainfall region over equatorial South America. SST in the western and central equatorial Atlantic ocean is a few degrees cooler than the western Pacific, as is seen in observations.

The relationship between the main variables along the equator at the end of each 20 year experiment is shown in Figs. 7 - 9. For $T_e = 24.5\ °C$ (Case I) precipitation is highest, pressure is minimum, SST maximum, and the thermocline deepest in the eastern Pacific, with westerly winds and currents over much of the Pacific. Conversely, for $T_e = 28.5\ °C$ (Case III) precipitation is highest, pressure is minimum, SST maximum, and the thermocline deepest in the western Pacific, with easterly winds and currents over much of the Pacific.

For the intermediate temperature $T_e = 26.5\ ^\circ C$ (Case II, Fig. 8) the SST, precipitation and thermocline depth maxima, associated with the eastward propagating coupled mode in the Pacific region, are in the eastern Pacific. Pressure is greatest over the central Pacific and secondary maxima in SST, precipitation and depth also occur in the west Pacific at this time. The sequence of events up to this time is as follows: the high rainfall region with associated locally convergent winds has moved to the east Pacific, leaving the central Pacific SST relatively cool. With the land and west Pacific SST warmer than the central Pacific, the easterly trade winds recover in the west and central Pacific, deepening the thermocline and increasing SST in the central and west Pacific. When SST increases sufficiently in the west Pacific another region of high rainfall develops there (Figs. 5 and 8 correspond to this phase) and subsequently propagates eastward, with the relationship between model variables like that described in Hirst and Lau (1989) for their mode B (model IV).

Case II thus shows some similarities with the observed ENSO cycle: warm water and precipitation build up in the west Pacific and move eastward. However the oscillation here is cyclic whereas in reality ENSO is a quasi-regular phenomena. Further, the persistence of warm SST and precipitation in the east Pacific for a few years is much longer than observed. This failure in the model may be related to the the absence of an annual cycle to which the termination of observed ENSO warm events is closely tied. (The effect of an annual cycle in land forcing only is described later.) By contrast, Case I is locked into a state resembling the warm phase of ENSO: precipitation, warm water, a shallow thermocline and westerly winds stretch across much of the equatorial Pacific.

The model displays three distinct modes of behaviour. For imposed land heating (Case III) the model development is dominated by the accompanying low-pressure and

high rainfall over the 'maritime continent' area, and disturbances in the west Pacific are unable to 'break off ' and travel independently eastwards. For land cooling (Case I), with weak westerlies across the Pacific and warm equatorial SST with little zonal contrast, the thermocline in the west Pacific cannot deepen to increase SST sufficiently and initiate a new event in the west Pacific. This contrasts with Case II where easterly winds are restored in the west Pacific when SST in the central Pacific falls substantially below that in the extreme west Pacific. This wind pattern then deepens the thermocline in the west Pacific which leads to the development of the next disturbance.

These results clearly illustrate the fundamental role of the 'maritime continent' in affecting the model behaviour.

Cases I-III use fixed $T_e$: the question arises as to whether variable $T_e$ could cause the events to occur irregularly? A further experiment, Case IV, has been carried out by simply adding an annual solar cycle to land heating. We set $T_e$ to vary with the day of the year, $D$, and latitude, $\phi$:

$$T_e = 22.5 + 6(1 - [\frac{(\phi - \phi_{sol})}{\phi_{max}}]^2) \tag{17}$$

where $\phi_{max}$ is the maximum latitude in the model (34 °) and the latitude of the solar maximum $\phi_{sol}$ varies with $D$:

$$\phi_{sol} = 23.3cos[\frac{2\pi(D - 170)}{360}]$$

giving solstices at days 10 and 350 in a 360 day year, and at equinox $T_e$ varies from 28.5 $°C$ at the equator to 22.5 $°C$ at the boundaries.

For Case IV the coupled disturbance became linked to the annual cycle, with a cycle

time of exactly 7 years (see Fig. 10). Examination of precipitation off the equator shows that rain moves across the equator following the maximum land heating. However, the interannual variability shows no signs of aperiodic behaviour.

In the following section we examine the model response to inclusion of shorter timescale atmospheric variability.

## EFFECTS OF SHORT-TIMESCALE FORCING

The model with neutral land produced regular oscillations, unlike the irregular oscillations observed, and the oscillations were still regular when an annual cycle was included. Another possible cause of irregular behaviour is atmospheric 'noise'. The atmospheric model used here has no intrinsic variability: for given constant forcing it reaches an identical steady state within about 15 days, regardless of intial conditions. We include 'noise' by adding a stochastic forcing to the atmospheric thermodynamic equation (7): Davey (1989) found that such forcing could produce intraseasonal waves in the form of moist Kelvin waves. Initially we hoped to investigate the effect of these intraseasonal waves on the interannual disturbances produced in the coupled model. However we found that when the present atmospheric model was run with stochastic forcing included, clear intraseasonal waves were not produced. This discrepancy is due to the form of background forcing $\theta_e$: in Davey (1989) $\theta_e$ was given a convenient smooth distribution; but for the present case the complex land geometry appears to inhibit the formation of the moist Kelvin waves. Nevertheless, we still considered it useful to investigate the response of the coupled model to shorter timescale (intraannual) forcing by repeating Case II with 'noise'.

For Case V the extra forcing was chosen to include a range of timescales including

and beyond the 40-50 day range, allowing the model to select its own preferred period of response (if any). Earlier work examining the effect of such forcing in a version of the model with no land, and with an ocean the size of the Pacific, has been reported in detail in Davey and Budin (1989).

The stochastic forcing term is $\epsilon\theta_R$ in Eqn. (7), where

$$\theta_R = [(1 - y/y_o)^2]\ A\ \Sigma_{k=1}^{2}\ \Sigma_{n=1}^{20} \cos\ [2\pi(kx/L - nt/\tau + \phi_{kn})], \qquad (18)$$

where $k$ and $n$ are zonal and temporal wavenumbers, $L$ is the length of the model domain (360° of longitude), $\tau$ is the maximum period of 180 days, and $\phi_{kn}$ is chosen randomly in the range 0 to 1. Thus the extra term has a discrete truncated white-noise spectrum covering periods from 9 to 180 days. The amplitude A is such as to give a peak value for $\theta_R$ of 2.8°C for the particular realisation (choice of $\phi$) used.

It is found that the interannual wave is not altered significantly by the additional high-frequency variability, neither in its growth stage nor at any time during its regular cycle. The 5 year time-longitude section of precipitation along 2°N in Fig. 11a (which should be compared with Fig. 2) shows that small perturbations are merely superimposed. Other atmospheric variables have similar behaviour, while high frequency disturbances in the ocean are less evident, with SST (Fig. 11b) being the least affected. The fluctuating winds do cause rapid changes in thermocline depth and ocean currents, but the ocean thermal timescale is such that SST responds very little to those oscillating changes.

The interannual wave tends to suppress the atmospheric response to $\theta_R$. The SST pattern due to the coupled interannual wave (which changes relatively slowly) is driving an atmospheric circulation with strong ascent over the warmest SST and

descent elsewhere, and this basic circulation inhibits the selective amplification of $\theta_R$ by moist processes.

## DISCUSSION AND CONCLUSIONS

The model used for this study is highly simplified: several important physical processes are absent or highly parameterised (eg higher modes in both component models, cloud-radiation feedbacks, atmospheric boundary layer processes, ocean radiative processes, evaporative cooling, topography etc ). As such it does not simulate the observed world particularly well and even at best the disturbances the model generates in the Pacific have a long timescale (3 years or more) which more closely match the return period of ENSO (2-7 years) than the time taken for warm water to shift eastwards from the western to central Pacific (several months). However it has been shown that the behaviour of this model is altered by land conditions, which fundamentally affect the development of the main precipitation areas. Such a link between land-processes (and in particular the Australasian monsoon) and ENSO has also been discussed by Anderson and McCreary (1985a and 1985b), Yamagata and Masumoto (1989), and Yasunari (1989). Further, for the neutral land case, the regeneration of the disturbance in the west Pacific is entirely by coupled model processes, which is consistent with the work of Hirst (1988). The delayed oscillator mechanism of Battisti (1988) for the Cane and Zebiak (1985) model is not operative here.

At the intermediate temperature ($T_e = 26.5°C$) Atlantic rainfall shows fluctuations of up to 50% which are in phase with rainfall in the eastern Pacific. This suggests some influence of ENSO on Atlantic rainfall, though a more complete model is best suited to studying such a link. However there is no globally circulating mode resembling the quasi-biennial mode of Yasunari (1985) and Rasmusson (personal communication). A single episode of such a mode is noted in the initial stages of the land heating case ($T_e = 28.5°C$). This is the only case for which the equatorial land masses are wet, indicating a possible role of land wetness in the quasi-biennial mode.

The lack of a mechanism to deepen the western equatorial Pacific thermocline in Case I is related to the prescribed cooling over the land to the immediate west. In Case II as the disturbance moves into the eastern Pacific easterly winds re-establish in the central and western Pacific due to the relative warmth of the land and far western SST compared to the cool central Pacific water. This shows the importance of the land/ocean heating contrast in the western Pacific and reinforces the results of Anderson and McCreary (1985a) who found it necessary to include land convection for their model to oscillate.

Fluctuations in Case II were regular, unlike observed ENSO events. Inclusion of a seasonal cycle in land heating, to add another timescale, merely shifted the interannual period to an integral number of years.

Results of experiments including random forcing show that in the present model it is difficult for short time scale fluctuations to affect interannual variability in the tropics, and in particular ENSO. The interannual waves depend on ocean-atmosphere coupling and latent heat release in the atmosphere, and changes to these require significant alterations of SST. In the experiment described here the high frequency variability in the atmosphere did not change SST sufficiently to disrupt interannual waves.

The results here should be treated with some caution however, as the model used here is clearly limited. Further experimentation with more 'intermediate' coupled models is necessary to understand more fully the effect of land convection and intraseasonal oscillations on ENSO.

**References**


Anderson, D.L.T. and J.P. McCreary, 1985a: Slowly propagating disturbances in a coupled ocean-atmosphere model. *J. Atmos. Sci.*, 42, 615-628.

Anderson, D.L.T. and J.P. McCreary, 1985b: On the role of the Indian ocean in a coupled ocean-atmosphere model of El Niño and the Southern Oscillation. *J. Atmos. Sci.*, 42, 2439-2442.

Battisti, D.S., 1988: Dynamics and thermodynamics of a warming event in a coupled tropical atmosphere-ocean model. *J. Atmos. Sci.*, 45, 2889-2919.

Battisti, D.S., 1989a: On the role of off-equatorial oceanic Rossby waves during ENSO. *J. Phys. Ocean.*, 19, 551-559.

Battisti, D.S., 1989b: Interannual variability in coupled tropical atmosphere-ocean models. *Phil. Trans. Roy. Soc.*, in press.

Battisti, D.S., and A.C. Hirst, 1989: Interannual variability in the tropical atmosphere/ocean system: influence of the basic state and ocean geometry. Sub, *J. Atmos. Sci.*

Budin, G.R., and M.K. Davey, 1989: A simple tropical coupled ocean-atmosphere model. *U.K. Meteorological Office Technical Note* , DCTN No. 75.

Davey, M.K. 1989: A simple tropical moist model applied to the '40 day' wave. *Quart. J. Roy. Meteor. Soc.*, 115, 1071-1107.

Davey, M.K. and G.R. Budin, 1989: Modelling Intraseasonal and Interannual variability in the tropics. *Phil. Trans. Roy. Soc.* , to appear.

Davey, M.K. and A.E. Gill, 1987: Experiments on tropical circulation with a moist model. *Quart. J. Roy. Meteor. Soc.*, 113, 1237-1270.

Gray, B.M. 1988: Seasonal frequency variations in the 40-50 day oscillation. *J. Climatology.*,8, 511-519.

Hirst, A.C., 1986: Unstable and damped equatorial modes in simple coupled ocean-atmosphere models. *J. Atmos. Sci.*, 43, 606-630.

Hirst, A.C., 1988: Slow instabilities in tropical ocean basin - global atmosphere models. *J. Atmos. Sci.*, 45, 830-852.

Hirst, A.C., and K.-M. Lau, 1989: Intraseasonal and interannual oscillations in coupled ocean-atmosphere models. Sub. to *J. Atmos. Sci.*

Lau, K.-M., 1985: Elements of a stochastic dynamical theory of the long-term variability of the El Niño / Southern Oscillation. *J. Atmos. Sci.*, 42, 1552-1558.

Lau, K.-M. and P.H. Chan, 1986: The 40-50 day oscillation and the ENSO: A new perspective. *Bull. Amer. Meteor. Soc.*, 67, 533-534.

Lau, K.-M. and P.H. Chan, 1988: Intraseasonal and interannual variations in tropical convection: A possible link between the 40 day mode and ENSO ?. *J. Atmos. Sci.*,45, 506-521.

Lau, K.-M., L. Peng, C.H. Sui, and T. Nakazawa, 1989: Dynamics of super cloud clusters, westerly bursts, the 30-60 day oscillation and ENSO: An unified view. *J. Meteor. Soc. Japan*,67, 205-219.

Lau, K.-M. and S. Shen, 1988: On the dynamics of the intra - seasonal oscillation and ENSO. *J. Atmos. Sci.*, 45, 1781-1797.

Mehta, A.V. and T.N. Krishnamurti, 1988: Interannual variability of the 30-50 day wave motions. *J. Meteor. Soc. Japan*,66, 535-548.

Philander, S.G.H. and E.M. Rasmusson, 1985: The Southern Oscillation and El niño. In *Adv. Geoph.* , 28a, 197-215.

Yamagata, T., and Y. Masumoto, 1989: A simple ocean-atmosphere model of the origin of a warm ENSO event. Sub. to *J. Meteor. Soc. Japan*

Yasunari, T., 1985: Zonally propagating modes of the global east-west circulation

associated with the Southern Oscillation. *J. Meteor. Soc. Japan*,63 , 1013-1029.

Yasunari, T., 1989: Impact of Indian Monsoon on the coupled atmosphere /ocean system in the tropical Pacific. Sub. to. *J. Climate.*

Zebiak, S.E. and M.A. Cane, 1987: A model El niño/Southern Oscillation . *Mon. Wea. Rev.*, 115, 2262-2278.

**Table 1. Parameters for the model ocean**

| | | |
|---|---|---|
| D | $1.44 \times 10^{-2}$ | Kg $m^{-2}sec^{-1}$ |
| g | 9.8 | m $sec^{-2}$ |
| $T_o$ | 17 | °C |
| $y_o$ | $3.44 \times 10^{6}$ | m |
| $\omega_o$ | $4 \times 10^{-7}$ | m $sec^{-1}$ |
| $\alpha$ | $2 \times 10^{-4}$ | $°C^{-1}$ |
| $\beta$ | $2.28 \times 10^{-11}$ | $m^{-1}$ $sec^{-1}$ |
| $\gamma$ | $3 \times 10^{-6}$ | m $sec^{-1}$ |
| $\delta_o$ | $2.74 \times 10^{-2}$ | $m^3$ °C $sec^{-1}$ |
| $\rho_o$ | $10^3$ | Kg $m^{-3}$ |
| $\nu_o$ | $2 \times 10^4$ | $m^2$ $sec^{-1}$ |

**Table 2. Parameters for the model atmosphere**

| | | |
|---|---|---|
| $E_o$ | $10^{-6}$ | $\text{sec}^{-1}$ |
| $E_v$ | $4 \times 10^{-7}$ | $\text{m}^{-1}$ |
| $H$ | $17000/\pi$ | m |
| $m$ | 235 | $^\circ\text{C m}^{-1}$ |
| $q_s(27)$ | $6.8 \times 10^{-2}$ | m |
| $\varepsilon$ | $4.4 \times 10^{-6}$ | $\text{sec}^{-1}$ |
| $\theta_{oo}$ | 310 | K |
| $(\theta_z)_{oo}$ | $3.89 \times 10^{-3}$ | $^\circ\text{C m}^{-1}$ |
| $\rho_{oo}$ | 1.225 | $\text{Kg m}^{-3}$ |
| $\nu_a$ | $10^5$ | $\text{m}^2\ \text{sec}^{-1}$ |

**Table 3. Summary of experiments**

| Experiment | $T_e$ °$C$ | $\theta_R$ | Description |
|---|---|---|---|
| I | 24.5 | 0. | Land cooling |
| II | 26.5 | 0. | Land neutral |
| III | 28.5 | 0. | Land heating |
| IV | Max 28.5 | 0. | Land forcing annual cycle |
| V | 26.5 | Max 2.8 | Land neutral and stochastic forcing |

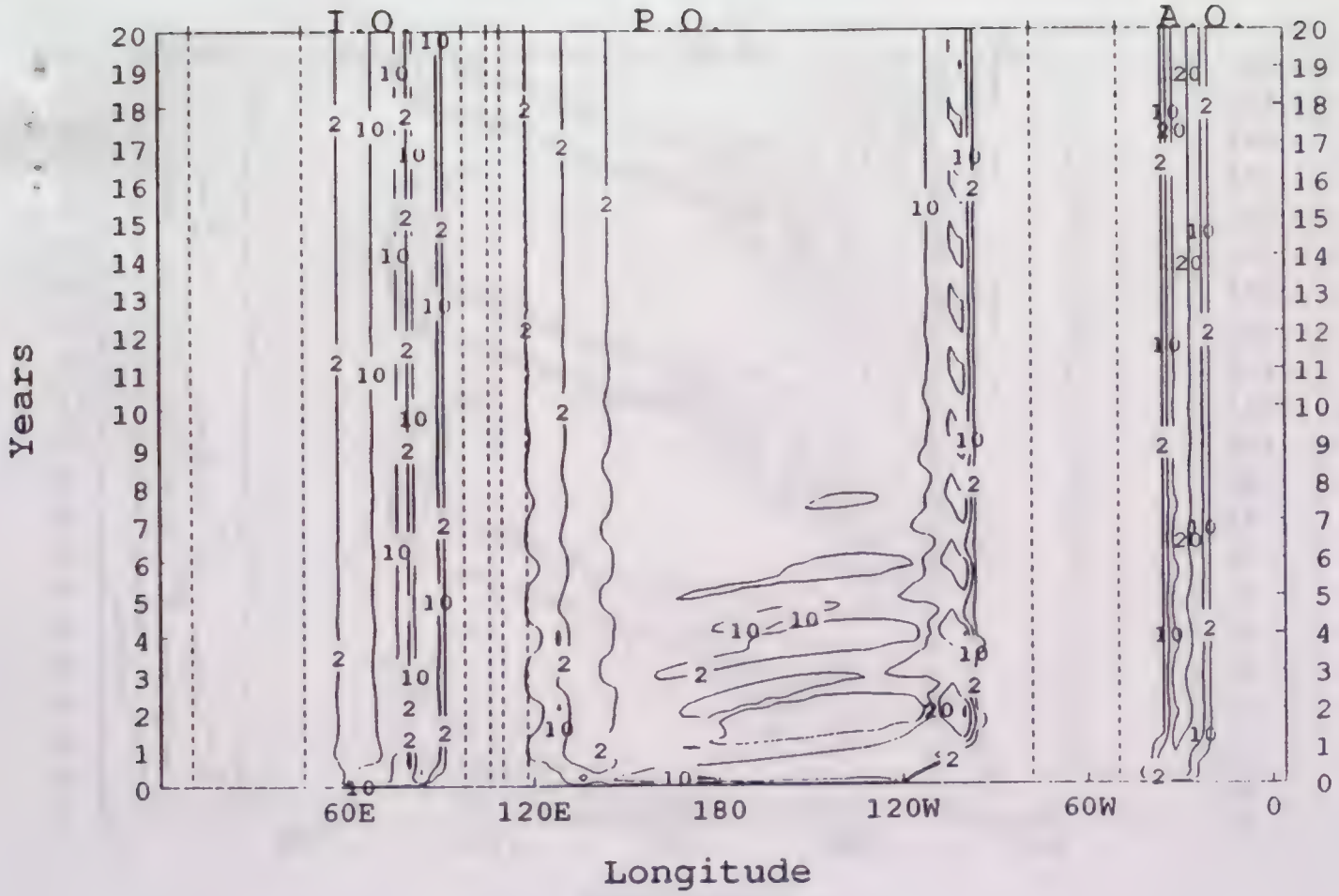


Fig. 1. Case I: Precipitation (mm/day) along 2°N for a 20 year experiment with land 'effective' temperature $T_e = 24.5°C$ giving cooling over land. Dashed lines indicate land/ocean boundaries. Contours at 2, 10, 20 , 30; maximum = 32.0 *mm/day*. I.O., P.O., and A.O. show the locations of the Indian, Pacific, and Atlantic oceans, respectively.

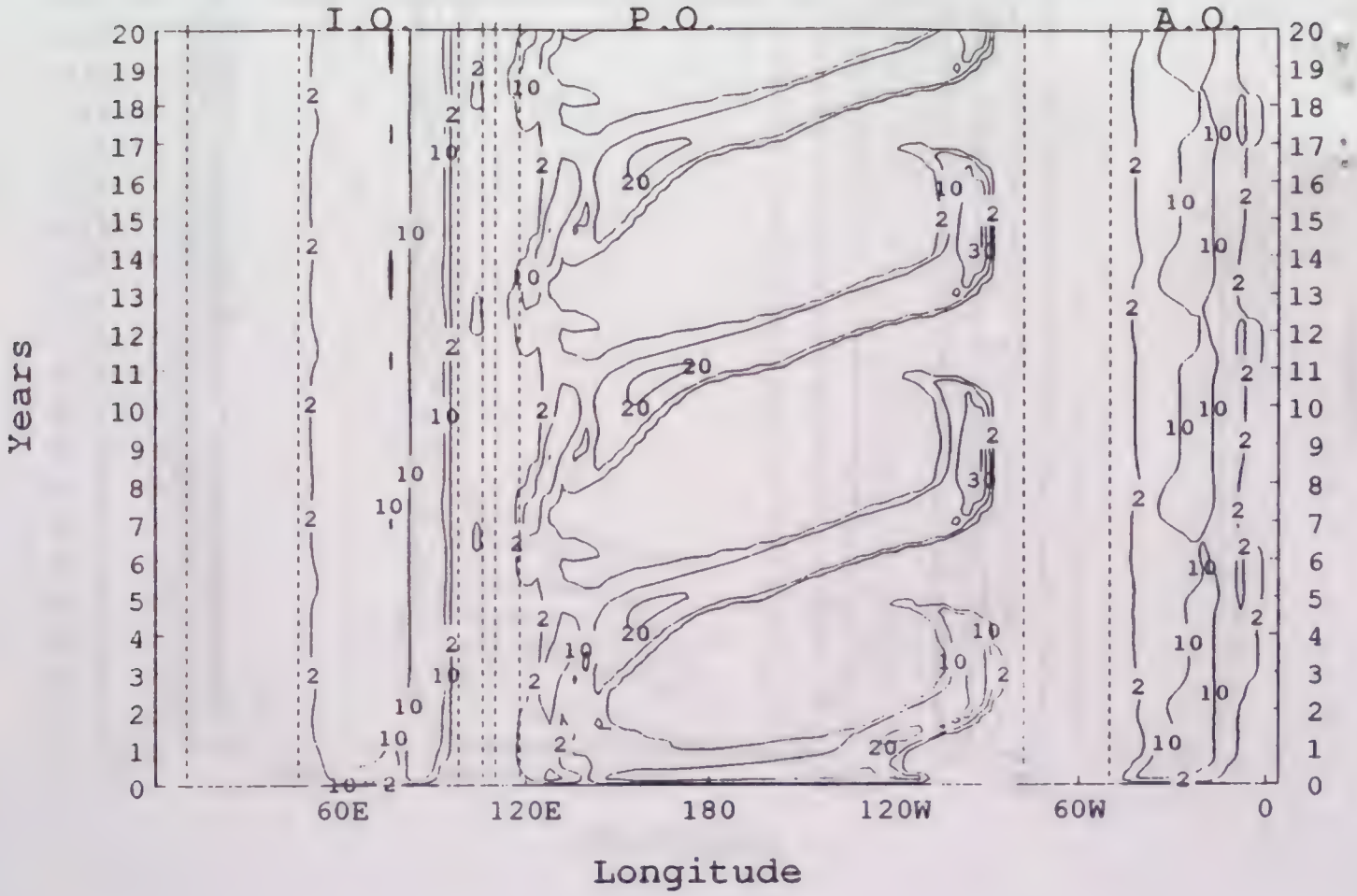


Fig. 2. Case II: As in Fig. 1 but for land 'effective' temperature $T_e = 26.5°C$ giving neutral land. Maximum = 30.4 $mm/day$.

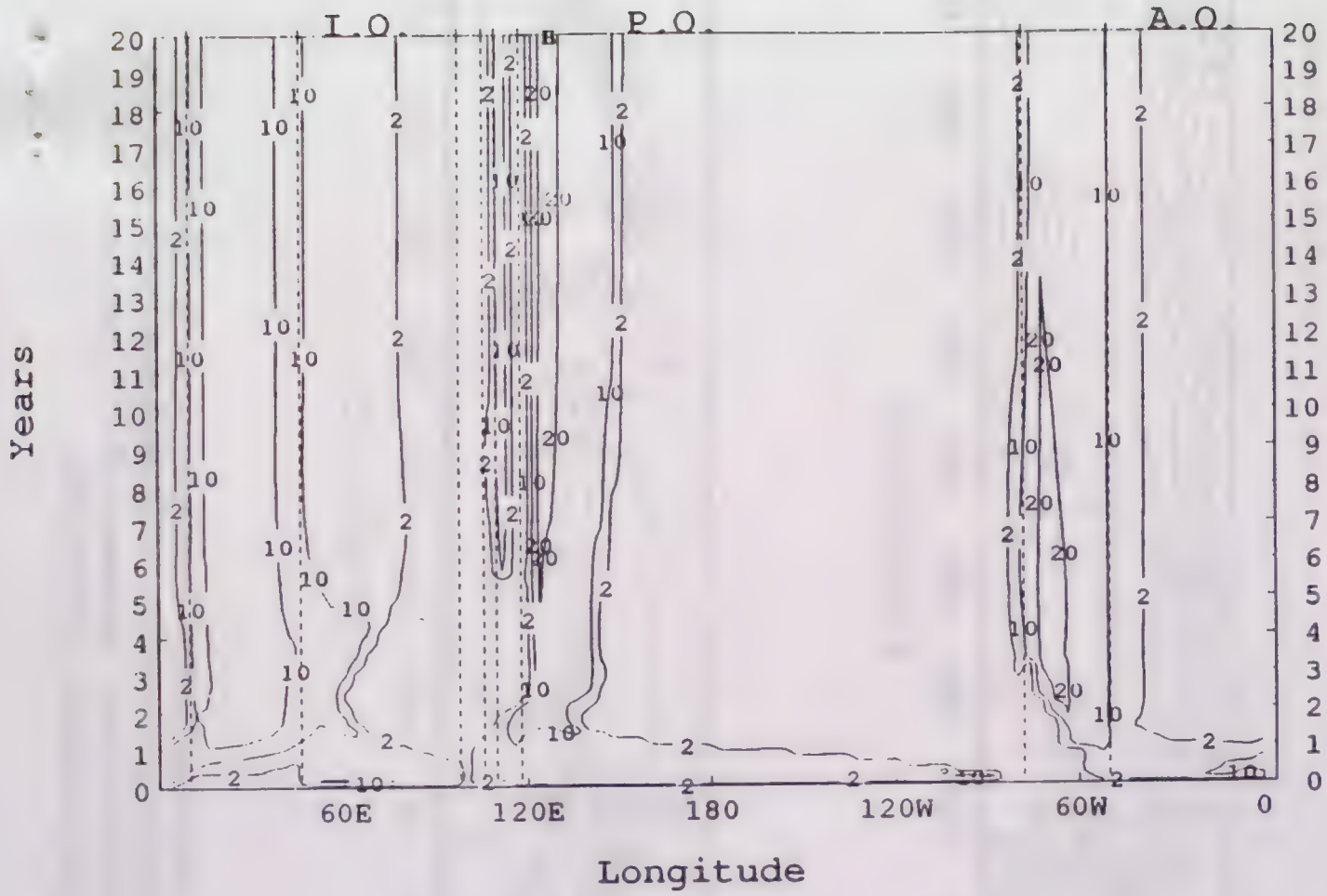


Fig. 3. Case III: As in Fig. 1 but for land 'effective' temperature $T_e = 28.5°C$ giving land heating. Maximum = 25.5 $mm/day$.

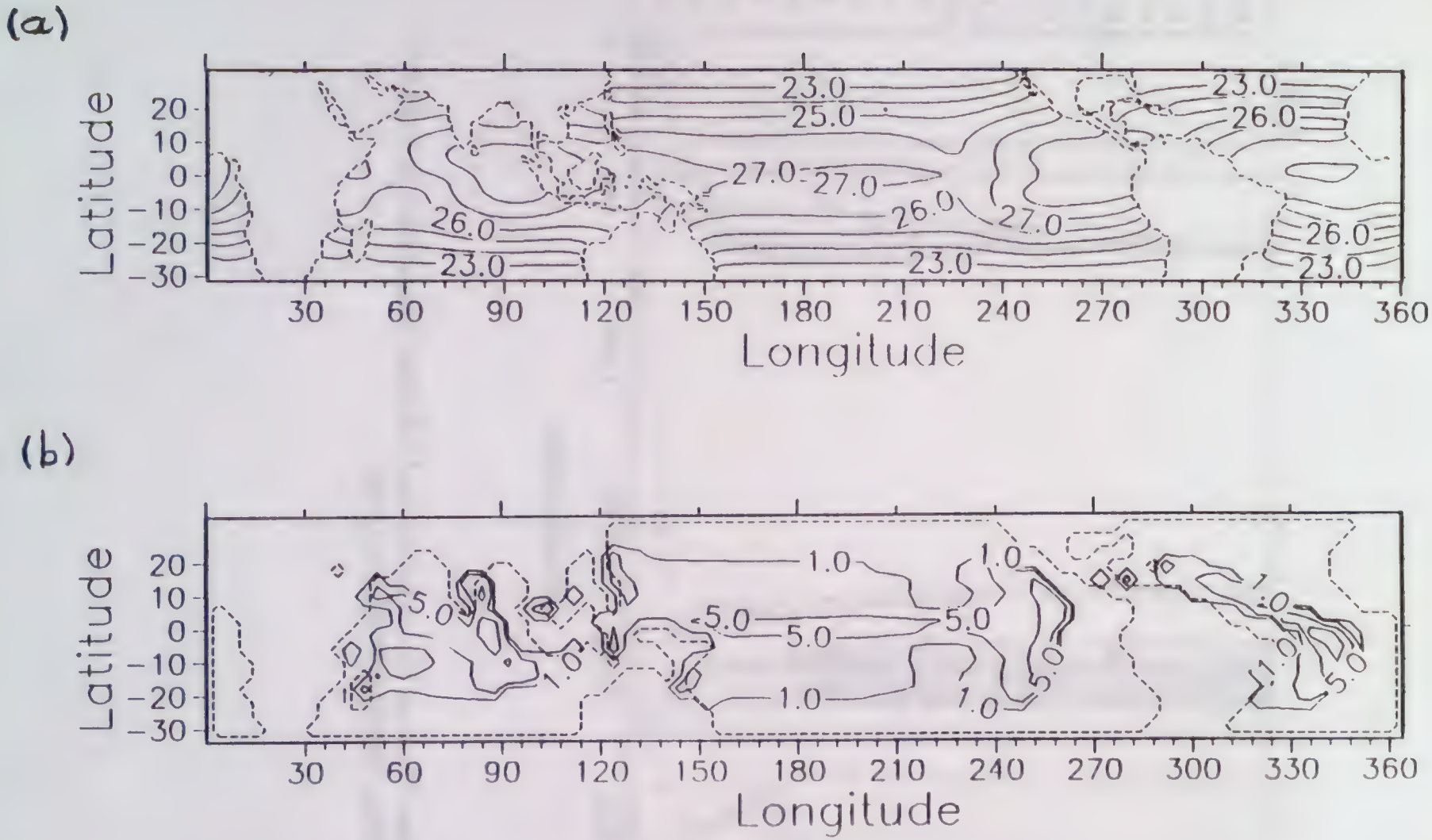


Fig. 4 Case I $T_e = 24.5°C$: (a) SST ($°C$) at the end of year 20. The continental outlines are dashed but note that the resolution of the ocean model is 1°by 1°whereas for the atmospheric model it is 4°by 4°. Minimum = 22.1 $°C$, maximum = 29.1 $°C$. (b) Precipitation ($mm/day$), maximum = 32.0 $mm/day$.

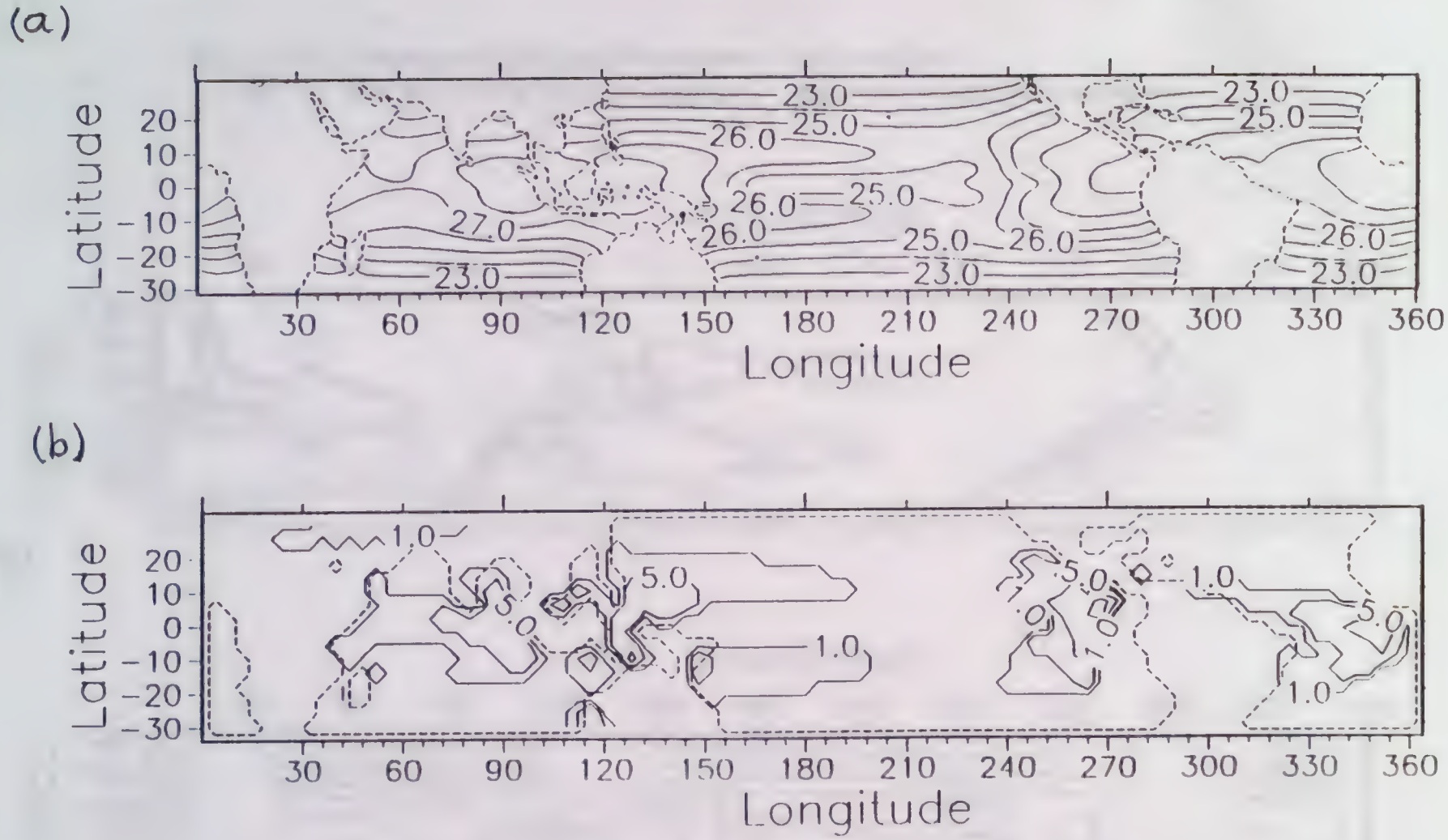


Fig. 5. Case II $T_e = 26.5°C$: (a) SST ($°C$). Minimum = 22.1 $°C$ maximum = 29.3 $°C$. (b) Precipitation ($mm/day$), maximum = 29.9 $mm/day$.

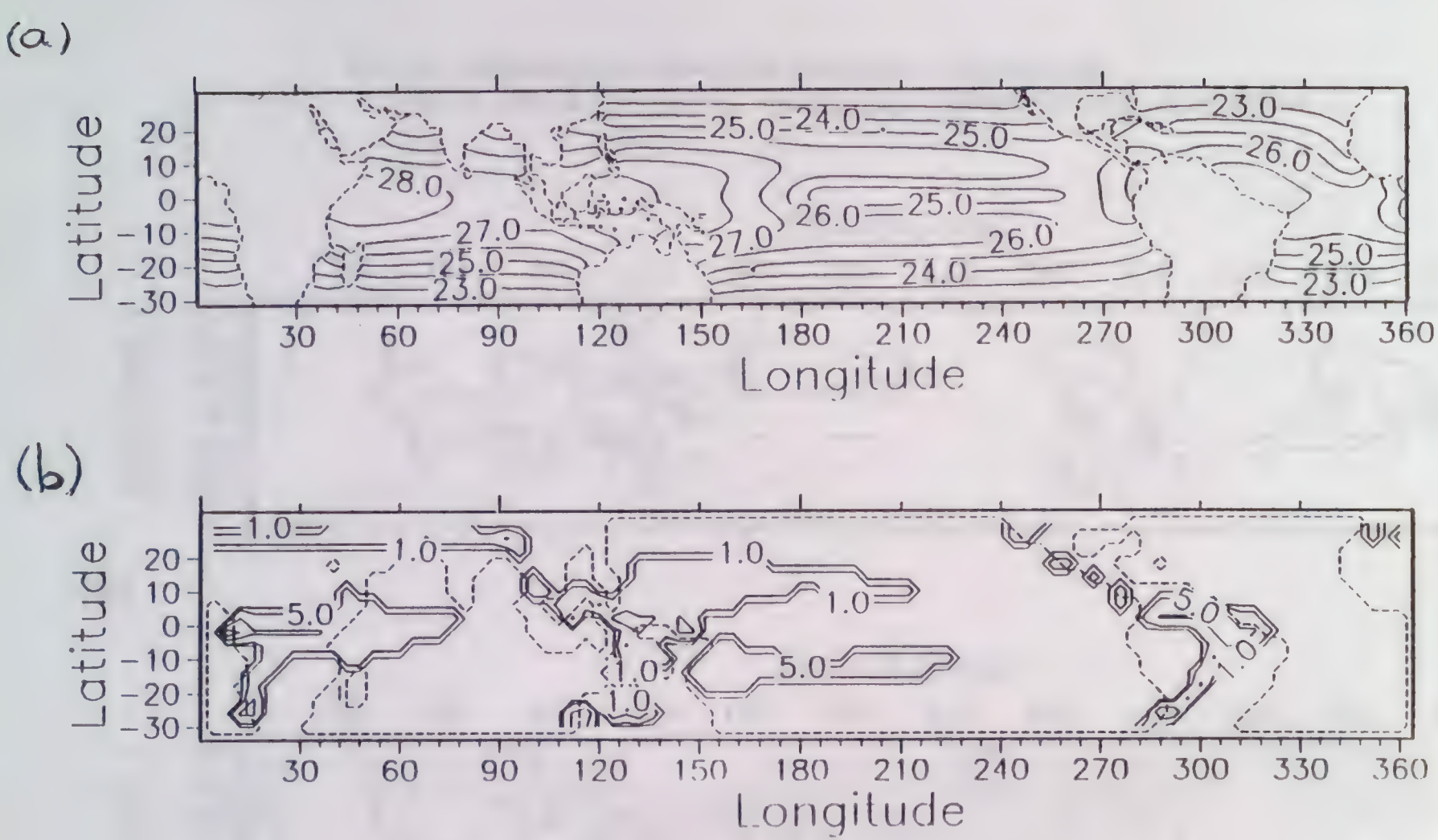


Fig. 6. Case III $T_e = 28.5°C$: (a) SST ($°C$). Minimum = 22.0 $°C$ maximum = 29.3 $°C$. (b) Precipitation ($mm/day$), maximum = 32.5 $mm/day$.

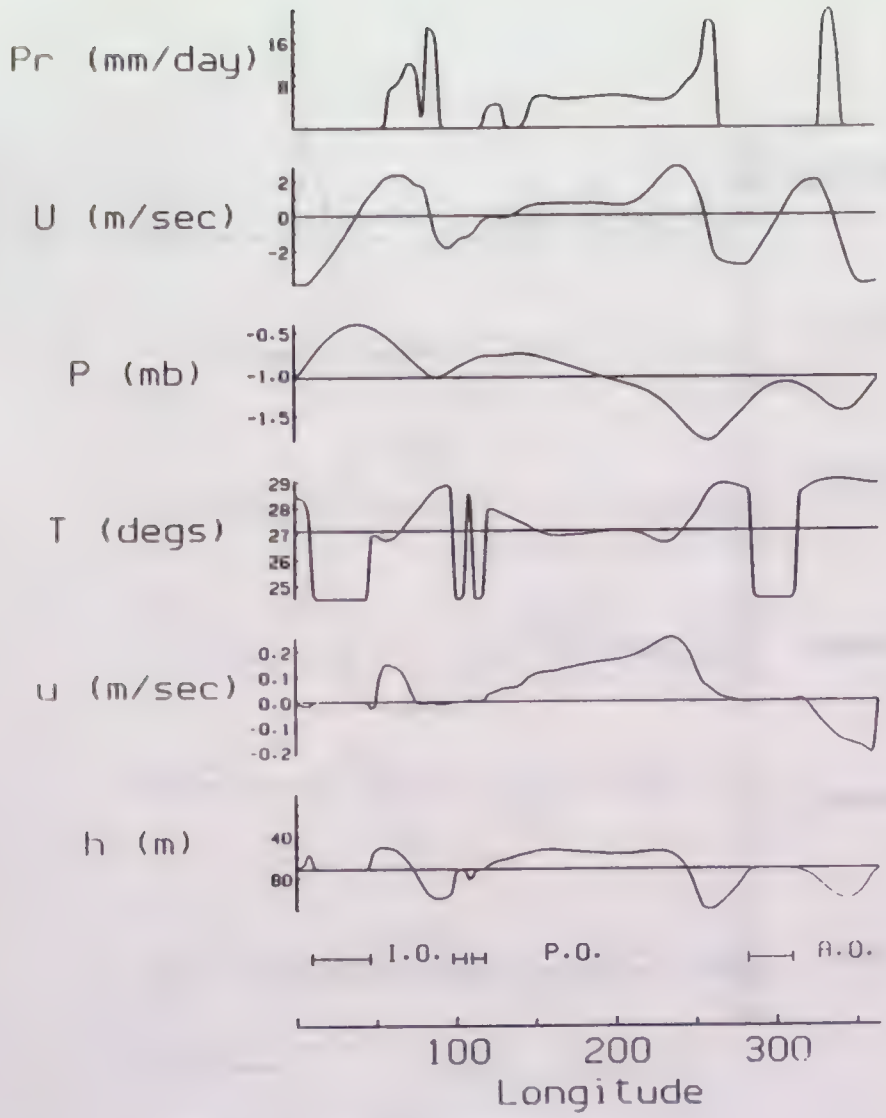


Fig. 7. Case I: Cross section of main model fields along 2°N at the end of year 20 for land 'effective' temperature $T_e = 24.5°C$. Fields are from top to bottom: precipitation (in $mm/day$), zonal wind ($m/sec$), pressure perturbation (in $millibars$), temperature ( $T_s$ in $°C$ and given by SST over ocean $T_e$ over land) ), zonal current ($m/sec$), and thermocline depth ($m$). The land configuration is indicated. Horizontal axes are set at zero for precipitation, zonal wind and zonal current, for other fields the axes are at the zonal mean value.

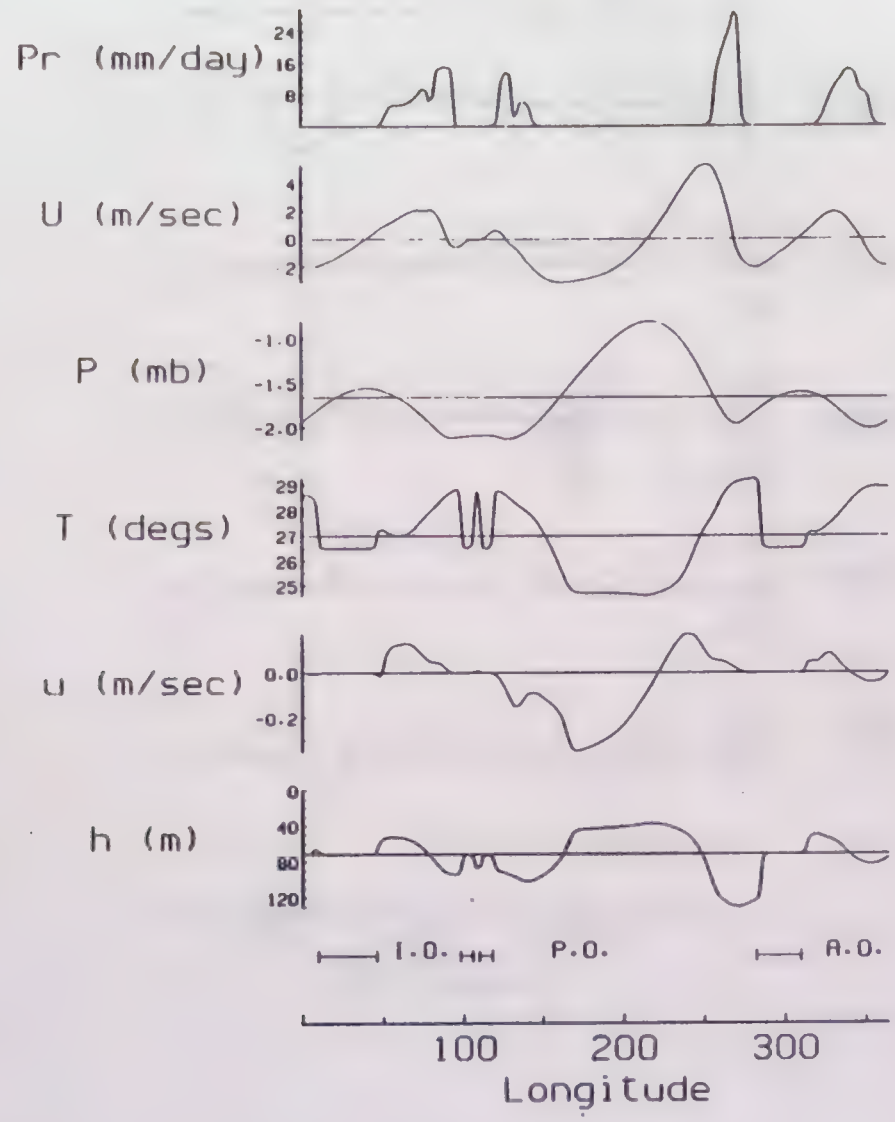


Fig. 8. Case II: As in Fig. 7 but for land 'effective' temperature $T_e = 26.5°C$.

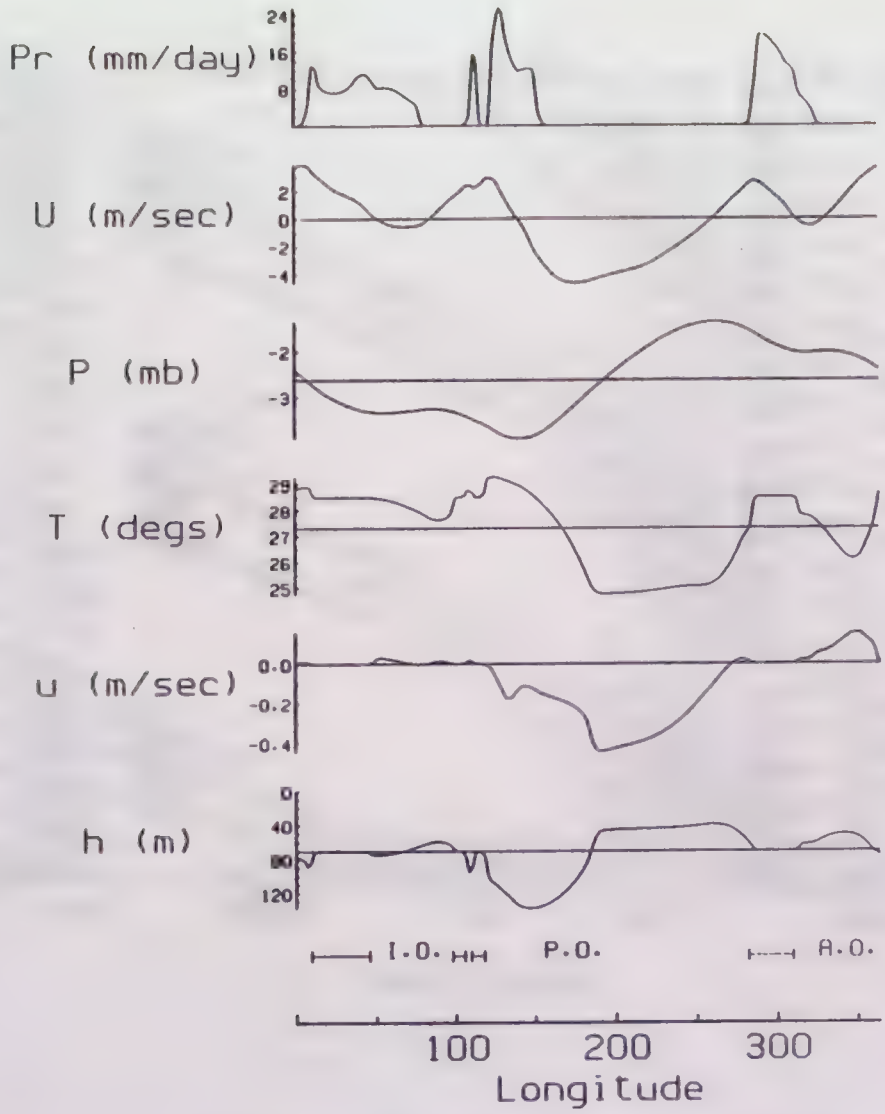


Fig. 9. Case III: As in Fig. 7 but for land 'effective' temperature $T_e = 28.5°C$.

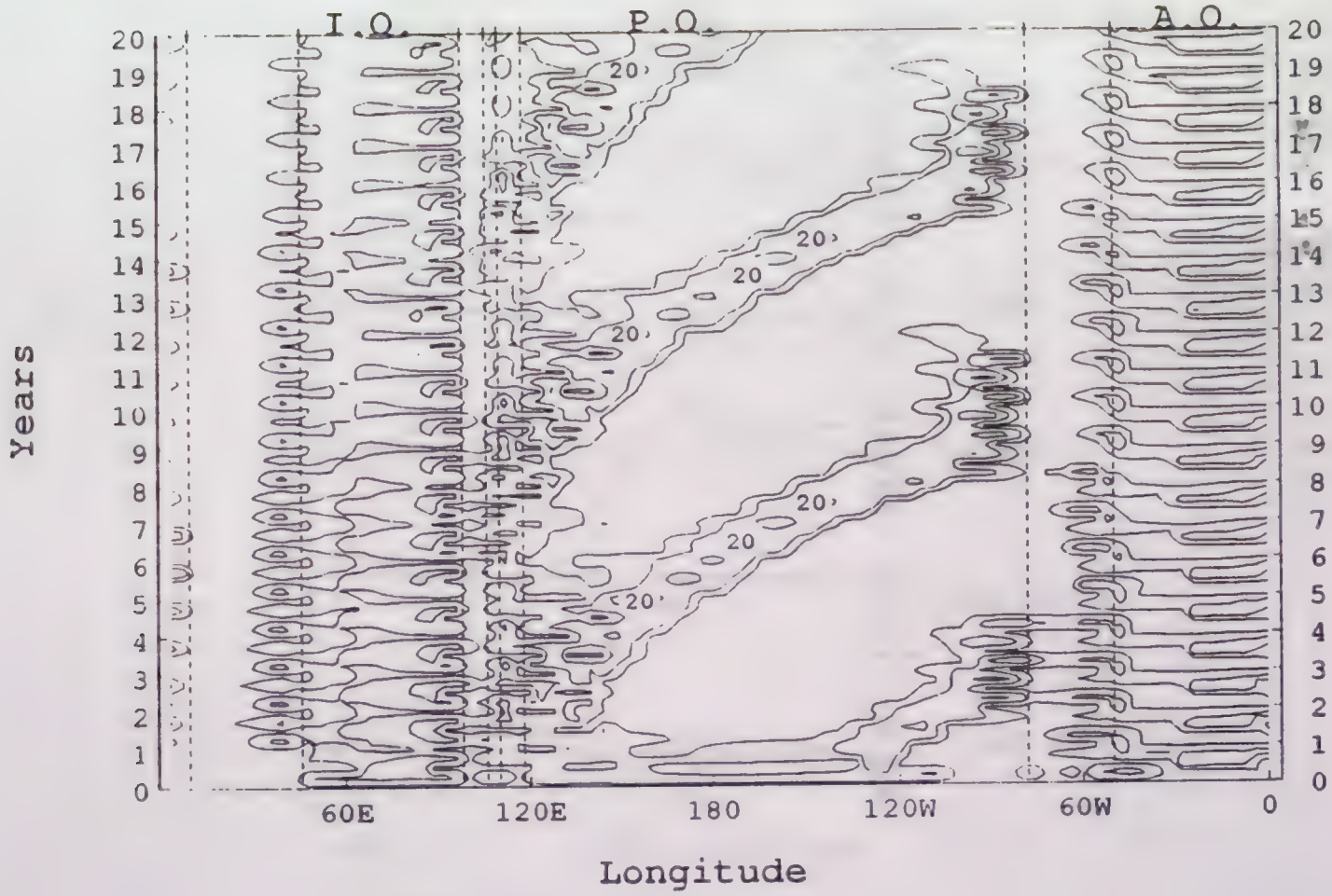


Fig. 10. Case IV: Precipitation ($mm/day$) along 2°N for coupled model including annual cycle in the land 'effective' temperature. Maximum = 34.2 $mm/day$.

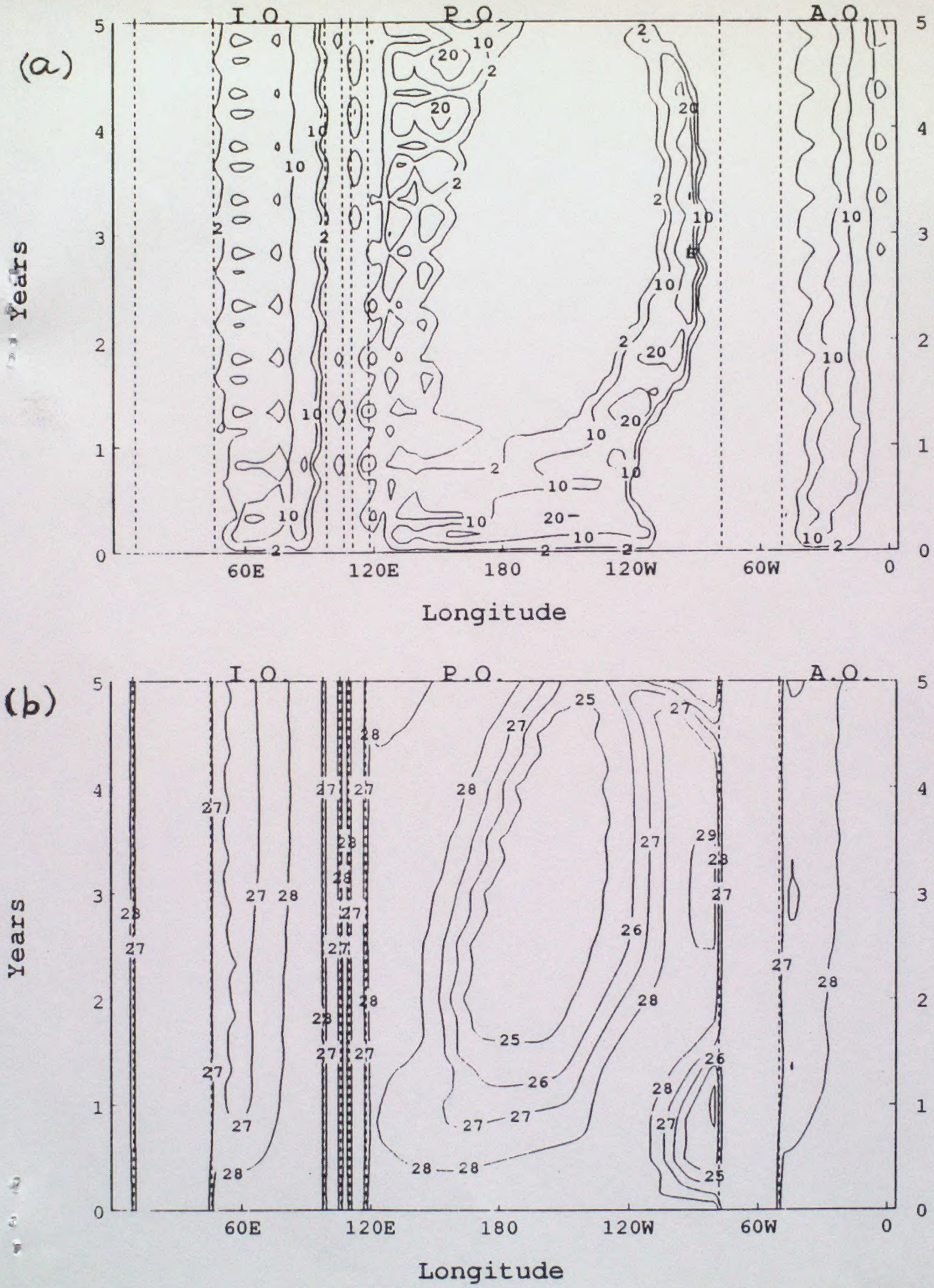


Fig. 11. Case V: (a) Precipitation ($mm/day$) along 2°N for coupled model including stochastic forcing. Maximum = 32.0 $mm/day$. (b) SST (°$C$). Minimum = 23.9 °$C$ maximum = 29.1 °$C$.

DYNAMICAL CLIMATOLOGY TECHNICAL NOTES

| | | |
|---|---|---|
| DCTN 1 | June 1984 | A scheme for incorporating the thermodynamic sea-ice model into a coupled ocean-atmosphere model.<br>C Cordon and M Bottomley |
| DCTN 2 | Sept 1984 | The parametrisation of the upper ocean mixed layer in coupled ocean/atmosphere models.<br>C Cordon and M Bottomley |
| DCTN 3 | Sept 1984 | The response of a simple thermodynamic sea-ice model to GCM forcing appropriate for perennial sea-ice.<br>M Bottomley |
| DCTN 4 | Sept 1984 | Potential vorticity in the stratosphere derived using data from satellites.<br>S A Clough, M S Grahame and A O'Neill |
| DCTN 5 | Sept 1984 | Simulation of the seasonal cycle of SST using globally specified climatological data to force simple ocean models.<br>M S Grahame |
| DCTN 6 | Sept 1984 | Development of an improved GCM radiation scheme.<br>A Slingo and R C Wilderspin |
| DCTN 7 | Sept 1984 | On the specification of surface fluxes in coupled atmosphere/ocean general circulation models.<br>J F B Mitchell, C A Wilson and C M Price |
| DCTN 8 | Sept 1984 | A survey of possible repercussions of the Soviet river reversal programme on Arctic sea-ice.<br>M Cattle |
| DCTN 9 | Oct 1984 | A study of a strong stratospheric warming during January 1982<br>T D A Fairlie |
| DCTN 10 | Nov 1984 | An intercomparison of the Met O 11 M45 model and the Met O 20 11-level model on the Cyber 205<br>J P Dyson |
| DCTN 11 | Nov 1984 | Simulation of observed time series of temperature and precipitation over eastern England.<br>D M Reed |
| DCTN 12 | Nov 1984 | Forecasts and analyses of the onset of the Southwest monsoon.<br>R Kershaw |
| DCTN 13 | Nov 1984 | On modelling the effects of $CO_2$ on climate.<br>J F B Mitchell |
| DCTN 14 | Dec 1984 | Development of a revised longwave radiation scheme for an atmospheric general circulation model.<br>A Slingo and R C Wilderspin |
| DCTN 15 | Jan 1985 | Rossby wavetrains in the stratosphere forced by localised disturbances in the troposphere.<br>C J Marks (Oxford), A O'Neill and V D Pope |

DYNAMICAL CLIMATOLOGY TECHNICAL NOTES

| | | |
|---|---|---|
| DCTN 16 | Jan 1985 | Observing system experiments using the Meteorological Office's 15-level model.<br>N A Bromley |
| DCTN 17 | Feb 1985 | Atmospheric general circulation simulation of the climate of the Mediterranean region.<br>M Cattle |
| DCTN 18 | Feb 1985 | Diurnal variation and cloud in a general circulation model.<br>C A Wilson and J F B Mitchell |
| DCTN 19 | Feb 1985 | The sensitivity of the Saharan region in a general circulation model.<br>W M Cunnington and P R Rowntree |
| DCTN 20 | Mar 1985 | The impact of aircraft observations on analyses and forecasts from the operational 15-level model.<br>R R Barwell |
| DCTN 21 | Mar 1985 | Non-linear effects on heat-induced circulation of the tropical atmosphere.<br>A E Gill and P J Phlips |
| DCTN 22 | Apr 1985 | Simulation of cloudiness with the U.K. Meteorological Office 11-layer AGCM.<br>A Slingo and R C Wilderspin |
| DCTN 23 | Apr 1985 | An integrated approach to the representation of cloud processes. R N B Smith |
| DCTN 24 | May 1985 | Nuclear Winter: Calculations of the shortwave radiative effects of soot aerosols.<br>A Slingo and P Goldsmith |
| DCTN 25 | Jul 1985 | Sea ice and the Antarctic winter circulation: a numerical experiment.<br>J F B Mitchell and T S Hills |
| DCTN 26 | Jul 1985 | A Budyko-Sellers model for study of ocean-atmosphere interaction.<br>W J Ingram |
| DCTN 27 | Aug 1985 | The effect of a shoaling thermocline on equatorially-trapped Kelvin waves.<br>A E Gill and B A King |
| DCTN 28 | Sept 1985 | $CO_2$ climate sensitivity and model dependence of results.<br>J F B Mitchell, C A Wilson and W M Cunnington |
| DCTN 29 | Sept 1985 | Handbook of the Meteorological Office 11-layer atmospheric general circulation model.<br>Volume 1 : Model Description<br>Edited by A Slingo |
| DCTN 30 | Sept 1985 | Impact of land surface variations on African rainfall in general circulation models.<br>P R Rowntree, M F Wilson and A B Sangster |

DYNAMICAL CLIMATOLOGY TECHNICAL NOTES

DCTN 31 Nov 1985 The annual cycle of sea level in the eastern tropical Pacific.
G R Rigg and A E Gill

DCTN 32 Nov 1985 An analytic model of the heat-induced tropical circulation in the presence of a mean wind.
P J Philips and A E Gill

DCTN 33 Nov 1985 The effect of resolution and diffusion on the simulated climate.
J F Dyson

DCTN 34 Jan 1986 Rossby adjustment over a step.
M K Davey, A E Gill, E R Johnson and P F Linden

DCTN 35 Jan 1986 Issues concerning the evaluation of effective surface roughness of heterogeneous terrain.
D J Carson

DCTN 36 Mar 1986 Climate sensitivity and past climates : evidence from numerical studies
J F B Mitchell

DCTN 37 Mar 1986 Parametrisations of land-surface processes in Meteorological Office numerical weather prediction and climate models
D J Carson

DCTN 38 Apr 1986 Modelling of land-surface processes and their influence on European Climate
D A Warrilow, A B Sangster and A Slingo

DCTN 39 Apr 1986 Simulation of climatic change due to increased $CO_2$
J F B Mitchell

DCTN 40 May 1986 On the interpretation of the Eliassen-Palm flux divergence. Part I : Theory
D G Andrews

DCTN 41 June 1986 Experiments on tropical circulation with a simple moist model.
M K Davey and A E Gill

DCTN 42 Jun 1986 Parameter regimes for studying isolated eddies.
P D Killworth and M K Davey

DCTN 43 Jun 1986 A comparison of the impact of an envelope orography and of a parametrisation of orographic gravity-wave drag on model simulations.
A Slingo and D W Pearson

DCTN 44 Jul 1986 The effect of a sea-surface temperature anomaly on a prediction of the onset of the south-west monsoon over India.
R Kershaw

DCTN 45 Jul 1986 An introduction to the parametrization of land-surface processes.
D J Carson

DYNAMICAL CLIMATOLOGY TECHNICAL NOTES

DCTN 46 Sept 1986 Lateral boundaries and the heat-induced flow in the tropical atmosphere.
P J Philips and A E Gill

DCTN 47 Nov 1986 Simulation of the diurnal cycle of outgoing longwave radiation with an atmospheric GCM.
A Slingo, R C Wilderspin and S J Brentnall

DCTN 48 Feb 1987 A 2 x $CO_2$ climate sensitivity experiment with a global climate model including a simple ocean
C A Wilson and J F B Mitchell

DCTN 49 Feb 1987 Sensitivity of the Met O 20 11-layer model to increased land surface roughness length
C C Heasman

DCTN 50 Feb 1987 The influence of atmospheric waves on the general circulation of the middle atmosphere
D G Andrews

DCTN 51 Feb 1987 Transport mechanisms in the middle atmosphere: an introductory survey
D G Andrews

DCTN 52 Mar 1987 The Met O 20 stratosphere-mesosphere model
M Fisher

DCTN 53 Apr 1987 Simulations of linear and nonlinear disturbances in the stratosphere
A O'Neill and V D Pope

DCTN 54 Apr 1987 Aspects of dynamics of the middle atmosphere inferred using data from a satellite and from a numerical model
T D A Fairlie and A O'Neill

DCTN 55 Apr 1987 The seasonal evolution of the stratosphere in the northern hemisphere
A O'Neill and V D Pope

DCTN 56 Apr 1987 The adjustment of numerical weather prediction models to local perturbations
B R Barwell and R A Bromley

DCTN 57 Jun 1987 Climate simulations for 9000 years before present: Seasonal variations and the effect of the Laurentide ice sheet
J F B Mitchell, N S Grahame and K J Needham

DCTN 58 Aug 1987 Climatic effects of nuclear war: the role of atmospheric stability and ground heat fluxes.
J F B Mitchell and A Slingo

DCTN 59 Oct 1987 The stratospheric major warming of winter 1984/85: observations and dynamical inferences.
T D A Fairlie and A O'Neill

DCTN 60 Oct 1987 Some comparisons between the middle atmosphere dynamics of the southern and northern hemispheres
D G Andrews

DYNAMICAL CLIMATOLOGY TECHNICAL NOTES

DCTN 61 Jan 1988 — Early winter in the northern stratosphere.
M N Juckes and A O'Neill

DCTN 62 Feb 1988 — Single column model tests of the Rowntree convection scheme using GATE data.
D Gregory

DCTN 63 Mar 1988 — The antarctic winter; simulations with climatological and reduced sea-ice extents.
J F B Mitchell and C A Senior

DCTN 64 Mar 1988 — An investigation of the Gates asynchronous coupling strategy using a simple energy-balance model.
D L Roberts

DCTN 65 Apr 1988 — The effect of improved physical parametrizations on simulations of cloudiness and the earth's radiation budget.
A Slingo, R C Wilderspin and R N B Smith

DCTN 66 May 1988 — Comparison of data and derived quantities for the middle atmosphere of the southern hemisphere.
W L Grose and A O'Neill

DCTN 67 Aug 1988 — Progress and future developments in modelling the climate system with general circulation models.
P R Rowntree

DCTN 68 Aug 1988 — A scheme for predicting layer clouds and their water content in a general circulation model.
R N B Smith

DCTN 69 Nov 1988 — Modelling climate change: an assessment of sea-ice and surface albedo feedbacks.
W J Ingram, C A Wilson and J F B Mitchell

DCTN 70 Dec 1988 — The "greenhouse" effect and climate change
J F B Mitchell

DCTN 71 Dec 1988 — On the dependence of climate sensitivity on convective parametrization.
W M Cunnington and J F B Mitchell

DCTN 72 Dec 1988 — Land surface parametrizations - basic concepts and review of schemes.
P R Rowntree

DCTN 73 Jan 1989 — Climate sensitivity: model dependence of results.
J F B Mitchell

DCTN 74 Jan 1989 — Parametrization of the upper ocean mixed layer in a tropical ocean GCM.
S Ineson and C Gordon

DCTN 75 Mar 1989 — A simple tropical coupled ocean-atmosphere model.
G R Budin and M K Davey

DYNAMICAL CLIMATOLOGY TECHNICAL NOTES

DCTN 76 Jun 1989 — The needs of general circulation models for runoff data.
P R Rowntree

DCTN 77 Jul 1989 — General circulation modelling of the atmosphere.
J F B Mitchell

DCTN 78 Jul 1989 — A model simulation of the seasonal cycle in the tropical Pacific Ocean using climatological and modelled surface forcing.
C Gordon and R A Corry

DCTN 79 Jul 1989 — Climatic impact of Amazon deforestation.
J Lean and D A Warrilow

DCTN 80 Sept 1989 — Surface evaporation during free convection.
C Gordon and D L Hunt

DCTN 81 Sept 1989 — A mass flux convection scheme with representation of cloud ensemble characteristics and stability dependent closure.
D Gregory and P R Rowntree

DCTN 82 Sept 1989 — The equilibrium response to doubling atmospheric $CO_2$.
J F B Mitchell